CD154 Tone Sets the Signaling Pathways and Transcriptome Generated in Model CD40-Pluricompetent L3055 Burkitt's Lymphoma Cells[1]

Ross Stewart,* Wenbin Wei,[2][†] Anita Challa,[2]* Richard J. Armitage,[‡] John R. Arrand,[†] Martin Rowe,[†] Lawrence S. Young,[†] Aristides Eliopoulos,[†] and John Gordon[3]*

Activated B cells reacting to small amounts of CD40L (CD154) maintain homeostasis by suppressing default apoptosis. Additional outcomes, particularly differentiation, demand higher CD40 occupancy. Here, focusing on survival, we compared changes in the transcriptome of pleiotropically competent, early passage L3055 Burkitt's lymphoma cells confronted with low (picomolar) and high (nanomolar) concentrations of CD154 to gain insight into how a single receptor sets these distinct phenotypes. Of 267 genes altering transcriptional activity in response to strong CD154 tone, only 25 changed coordinately on low receptor occupancy. Seven of the top nine common up-regulated genes were targets of NF-κB. Direct measurement and functional inhibition of the NF-κB pathway revealed it to be central to a CD40-dependent survival signature. Although the canonical NF-κB axis was engaged by both signaling strengths equally, robust alternative pathway activation was a feature selective to a strong CD40 signal. Discriminatory exploitation of the two separate arms of NF-κB activation may indicate a principle whereby a cell senses and reacts differentially to shifting ligand availability. Identifying components selectively coupling CD40 to each axis could indicate targets for disruption in B cell pathologies underpinned by ectopic and/or hyper-CD154 activity such as neoplasia and some autoimmunities. *The Journal of Immunology,* 2007, 179: 2705–2712.

The CD40-CD154 interaction represents a pivotal receptor-ligand pairing at several junctures in a B cell response to T-dependent Ag. During the complex germinal center (GC)[4] phase, signals delivered through CD40 may impact survival, Ig class-switch recombination, Ag-presenting capacity, selection, affinity maturation, and differentiation to memory and/or plasma cells (1). The choice between these assorted outcomes can be informed not only by the maturation stage-specific status of the B cells but also by the duration and strength of interaction between CD40 and ligand (1).

CD40-CD154 pairing has typically been considered paracrine. There are scenarios, however, where B cells produce and use CD154 in autocrine mode (2, 3). Such a phenotype could underpin certain B cell pathologies: lymphomas of GC origin contributing key examples. Both large B cell lymphoma and Burkitt's lymphoma (BL) have been shown to exploit autonomous CD154 for

survival (2, 4). For BL cells, CD154 mRNA is turned on in response to population depletion, the very low amount of ligand produced being used to reverse otherwise spontaneous apoptosis (2). A recent study suggests that such cell-autonomous behavior might recapitulate normal homeostasis where polyreactive B cells are maintained by CD40-dependent signals received from naive CD4 T cells constitutively expressing sparse, but functionally vital, CD154 at their surfaces (5).

We have previously shown how early passage, biopsy-like BL cells surviving in response to exceptionally low (picomolar) amounts of CD154 do so without discernible alteration in levels of either anti-apoptotic Bcl-x_L or Bcl-2, or proapoptotic Bax (2). Moreover, by comparison with strong CD40 signaling where markers of both cellular activation and differentiation develop, BL cells receiving a weak CD40 signal retain their characteristic GC phenotype. The functional pleiotropy of the lymphoma cells models the behavior of physiological B cell counterparts confronted with graded levels of CD154 (1).

In the present study, we have exploited the CD40-pluricompetent L3055 BL clone (2, 6) to: 1) explore how a single receptor interprets different levels of occupancy to deliver restricted or multiple outcomes in the same target cell; 2) identify key pathways and components through which low-level engagement of CD40 engenders survival. The hope is that by determining a gene signature and/or signal transduction cascade that is selectively responsible for installing a CD40-dependent survival phenotype, we may in turn indicate candidate targets for disruption where this outcome is excessively, or inappropriately, active; as in, for example, certain B cell malignancies and/or B cell-associated autoimmunities.

Materials and Methods

Cell lines and reagents

The EBV-negative BL cell line L3055 was derived and maintained in early passage (<80) as were stable *bcl*-2 and *bcl*-x_L transfectants and subclones containing empty vector; (2, 6). Recombinant soluble trimeric human

[4] Abbreviations used in this paper: GC, germinal center; BL, Burkitt's lymphoma; sCD154, recombinant soluble trimeric human CD40L; cIAP2, cellular inhibitor of apoptosis protein.

CD40L (sCD154) was as described (2). SC-514 was purchased from Calbiochem. FITC-conjugated murine mAbs were: Ki-24 (IgG3; BD Pharmingen) to CD70; DX2 to CD95; and 6.5B5 to CD54 (both IgG1; Dako).

Affymetrix microarray analysis of gene expression changes

RNA, 10 μg, isolated using TRIzol, together with a HPLC-purified GENSET T7 (dT)$_{24}$ primer (Helena Biosciences) and Superscript Double Stranded cDNA Synthesis Kit (Invitrogen Life Technologies) were used to generate cDNA. cDNA, isolated by extraction with phenol-chloroform-iodoacetamide (Ambion), was used to produce biotin-labeled cRNA via the Enzo BioArray High Yield Transcription Labeling Kit (Enzo Life Sciences). cRNA, 25 μg, was fragmented and hybridized to the human genome focus array (Affymetrix) as per the Affymterix protocol. Arrays were washed and stained using a combination of streptavidin PE (Molecular Probes) and biotinylated anti-streptavidin (Vector Laboratories). Washing and staining were conducted using the Fluidics Station (Affymetrix) as per the manufacturer's instructions. Stained arrays were scanned using a model 2500 microarray scanner (Affymetrix), and data quality was assessed using MAS 5.0 report files.

Scanned images of microarray chips were analyzed using probe level quantile normalization (7). Subsequently, robust multiarray analysis on the raw cell intensity files was performed using the Affymetrix package of the Bioconductor (http://www.bioconductor.org) project (8). The results of this analysis and full details of the experimental procedures can be found in the MIAME Express database (http://www.ebi.ac.uk/miamexpress/), accession number E-MEXP-1113. Differentially expressed probe sets were identified by a paired analysis of the expression values using the Significance Analysis of Microarrays (9). Differentially expressed probe sets common to both treatments were identified using Access (http://www.microsoft.com/access). Images for presenting data were generated using Genesis (http://www.genome.tugraz.at/Software/GenesisCenter.html).

Semiquantitative and real-time RT-PCR

Five micrograms of total RNA, isolated using Trizol, were used to synthesize cDNA via SuperScript II (Invitrogen Life Technologies). PCR amplification was performed using AmpliTaq Gold (Applied Biosystems) with primers at 1 μM and Mg^{2+} at 1.5 mM. Temperature cycling on a DNA Engine TetTrad (MJ Research) used the following conditions: 95°C for 10 min; 30 cycles of 95°C for 30 s; annealing for 30 s and 72°C for 2 min. β-Actin was used as a housekeeping gene for sample normalization. Products taken from the exponential phase of reactions were analyzed by ethidium bromide gel electrophoresis and identified by fragment size. Densitometric analysis was conducted using Gene Tools.

Primer sequences, amplicon size and annealing temperature for *CIAP2*: forward 5′-GGTGGACTCAGGTGTTGGG-3′, reverse 5′-AAAATG GATAATTGATGACTCTGC-3′, 204 bp, 60°C; 50 μl real-time RT-PCR were ran in 96-well optical reaction plates on an Applied Biosystems 7900HT Fast Real-Time PCR System. Reactions contained 5 μl of cDNA, TaqMan Universal PCR Master Mix, and Assays-on-Demand Gene Expression Assays, according to manufacturer's instructions. Assays and their targets were: *CIAP2* (Hs00154109_m1), *A20* (Hs00234712_m1) *BCL6* (Hs00153368_m1), β-*ACTIN* (Hs99999903_m1). Data were analyzed using SDS version 2.2.

Immunodetection of cellular inhibitor of apoptosis protein (cIAP2) and NF-κB subunits

Whole cell, nuclear and cytoplasmic lysates were prepared as elsewhere (6). Protein concentration was determined and equal amounts from each lysate separated by SDS-PAGE. Separated proteins were transferred to Imobilin P membrane (Millipore). Membranes were blocked in 10% nonfat milk and probed with rabbit anti-human p65 (C20; 1/1000), rabbit anti-human cIAP2 (H-85; 1/2000; Santa Cruz Biotechnology); mouse anti-human p100/p52 (005-361) (1/500; Upstate Biotechnology); mouse anti-human β-actin (AC-15; 1/10,000; Sigma-Aldrich). Abs were diluted in TBS containing 1% Tween and 5% nonfat milk powder. Membranes probed with anti-human p100/p52 were blocked using 5% nonfat milk. Immunoblots were visualized using HRP-conjugated secondary Abs and a chemiluminescence detection system.

Results

Transcriptional profiling to assist discrimination of pathways specifying distinct CD40-dependent phenotypes with a focus on survival

We previously found (against our own expectations) that change in neither Bcl-x$_L$ nor Bcl-2 was essential to the CD40-dependent survival of L3055 biopsy-like BL cells retaining a GC phenotype (2). Subsequent studies indicated the same for phosphoinositide-3′-kinase (PI-3K) activity with low level, survival-promoting concentrations of CD40L failing to augment the phosphorylation of Akt: a downstream target of and surrogate readout for PI3K activity (Refs. 10 and 11 and A. Challa, R. Stewart, and J. Gordon; unpublished data). We therefore turned to gene expression profiling to assist the search for alternative candidates, essentially asking whether a survival signature might be disclosed by way of an overlapping set of gene changes common to low- and high-level CD154 encounter, both protecting from apoptosis but with the latter additionally driving activation and differentiation (2, 6).

Gene expression changes in L3055 cells resulting from CD40 signaling. Total RNA isolated from L3055 cells was subjected to microarray analysis. Genes whose expression changed at 6h with sCD154 at 2 μg/ml and 2 ng/ml in three independent experiments were identified by a paired analysis of the expression values using the Significance Analysis of Microarrays software. This analysis set a 1.4-fold change threshold relative to the level seen in untreated cells and a false discovery rate of ≤5% when identifying genes that showed a changed level of expression. Full results of said analysis can be found online as supplemental data.

We first scrutinized the microarray data obtained from L3055 cells in this study ranking target genes with respect to having received a strong CD40 signal. Treatment of L3055 cells with 2 μg/ml sCD154 resulted in the up-regulation of 215 transcripts, *CD54/ICAM1* showing the greatest change (7.8-fold). Only 52 transcripts were down-regulated, the largest change here being the *AID* gene (3.1-fold). To assist interpretation, the 267 genes showing altered expression with a strong CD40 signal were grouped into distinct clusters of biological function using the gene ontology data from the Nettaffx Analysis Centre. A selection of these genes and their changes relative to untreated cells are shown in Fig. 1. Changes at low signal strength are included for comparison.

Unsurprisingly, a significant proportion of the genes impacted by strong CD40 signaling are involved in the immune response (Fig. 1). Approximately one-half of the genes in this subset are engaged in Ag-processing/presentation including several MHC genes, subunits implicated in the formation of the immunoproteasome, a component of the TAP transporter and the TAP-binding protein, tapasin. Also up-regulated were the T cell costimulators 4-1BB-L (1.5-fold) and CD83 (2-fold). Among the TNF/TNFR family, CD70/TNFSF7 showed a 3.3-fold up-regulation whereas its receptor CD27/TNFRSF7, a centrocyte/memory cell marker (12), showed down-regulation (1.8-fold); CD95/TNFRSF6/FAS, a well-established CD40 signature, registered a 2.4-fold increase; *lymphotoxin-β* (*LTB*) and *lymphotoxin-α* (*LTA*) were similarly up-regulated, 2-fold and 1.5-fold, respectively. With respect to GC biology, two notable changes were a 1.8-fold down-regulation of the transcription repressor BCL6 (13) and the 3.1-fold down-regulation of *AID* (activation-induced cytidine deaminase) being intimately involved in class switch recombination and somatic hypermutation (14).

Another cluster of genes targeted by strong CD40 signaling in L3055 cells links to proliferation. This includes down-regulation (1.5-fold) of cell division cycle 25B (CDC25B) and up-regulation (2.2-fold) of the cyclin-dependent kinase inhibitor CDKN1B/P27KIP1 (Fig. 1). Both *IRF1* and *IRF2* were up-regulated after a strong CD40 signal. The IRF1 protein can inhibit growth in cell lines whereas IRF2 has been characterized as an antagonist of IRF1 (15). *Activating transcription factor 5* (*ATF5*) was up-regulated 2.4-fold: though its function here is unclear, the product of
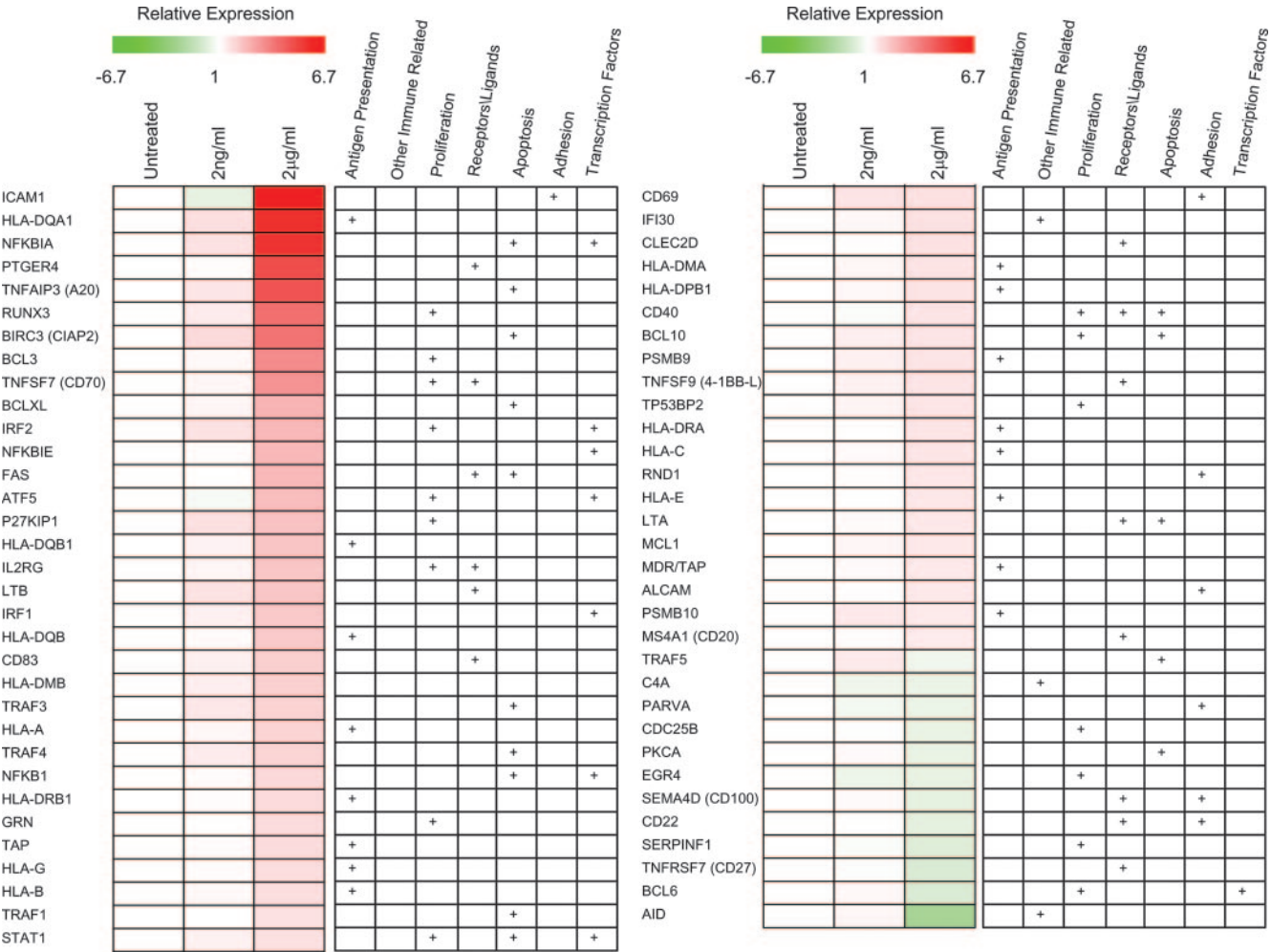
FIGURE 1. Gene expression changes in L3055 cells after 6 h of exposure to sCD154, and their functions. Expression profiling was performed on L3055 cells cultured at 10^6/ml for 6 h with 0 or 2 ng or 2 μg/ml sCD154. Gene expression changes identified after analysis of three independent experiments were classified by function using gene ontology data from the Nettaffx Analysis Centre. Heat maps represent the changes in expression for a selection of identified genes in treated relative to untreated cells. Red indicates an up-regulation; green represents a down-regulation. The functions of the identified genes are indicated to the right of each heat map. Forty-two identified genes were associated with the immune response and have been subdivided into four functions; those involved in Ag processing and presentation, surface receptors and ligands, transcription factors, and other immune related molecules. Of the identified genes, 17 were associated with the control of proliferation, 7 with adhesion, and 16 with the process of apoptosis. Expression changes following treatment with 2 ng/ml sCD154 are shown for comparison, but in most cases are not significant.

ATF4, a closely related gene, has been shown to repress transcription from the cyclin A promoter (16). *Early growth response 4 (EGR4)* was down-regulated 1.5-fold: this gene has been positively linked to proliferation (17). The direction of these changes is consistent with the growth-inhibitory phenotype engendered in BL cells on high-level CD40 occupancy (6). Several genes involved in adhesion also showed altered expression following a strong CD40 signal (Fig. 1).

A cluster particularly relevant to the present study comprised genes involved in controlling apoptosis (Fig. 1). *BIRC3/CIAP2* is discussed in *Gene expression change common to weak and strong CD154 tone*. Two established CD40 targets of the Bcl-2 family, *MCL1* and *BCL2L1/Bcl-Xl*, were up-regulated 1.5-fold and 2.5-fold respectively. Several genes within this subset are involved in signaling pathways that impact apoptosis; including via CD40 itself. Transcripts encoding four members of the TRAF family of adaptor molecules altered expression level in response to a strong CD40 signal: *TRAF1*, *TRAF3*, and *TRAF4* showing up-regulation (1.6-fold to 1.9-fold); *TRAF5* showing a 1.7-fold down-regulation. Also registering were targets the products of which impact, in turn,

on the transcriptional control of genes that regulate apoptosis, e.g., NF-κB pathway components (see *Gene expression change common to weak and strong CD154 tone*) and the *STAT1* transcription factor.

Gene expression change common to weak and strong CD154 tone. Of the 267 transcripts registering a response to CD154 at 2 μg/ml, only 25 changed in cells receiving a weak CD40 signal (Table I). Among the 20 shared up-regulated genes, 7 were NF-κB targets including components of the pathway itself such as the negative regulators A20/TNFAIP3 and IKBA/NFKBIA, as well as the positive regulator TANK (TRAF family member-associated NFKB activator) (18, 19); the zinc finger protein A20 directly confers resistance to apoptosis in B lymphoma cells (20).

The shared gene showing the greatest up-regulation (1.8-fold) following a weak CD40 signal was the NF-κB target *CIAP2/ BIRC3*. Previously identified as a major CD40 target gene in tonsillar B cells (21), its product (a member of the antiapoptotic inhibitor of apoptosis family of proteins) interacts directly with TRAF2 following CD40 ligation (22). Another NF-κB target

Table I. *Differentially expressed genes common to weak (2 ng/ml sCD154) and strong (2 μg/ml sCD154) signals in L3055 cells compared with control*

Gene	Description	Mean Fold Change	
		Weak	Strong
BIRC3[a]	Baculoviral IAP repeat-containing 3	1.78	4.08
TANK[a]	TRAF family member-associated NFKB activator	1.73	3.42
HLA-DQA1/HLA-DQA2	MHC class II, $DQ_{\alpha 1}$ or $DQ_{\alpha 2}$	1.66	5.79
PIM1[a]	*pim-1* oncogene	1.64	3.25
NFKBIA[a]	NF-κ light polypeptide gene enhancer in B cell inhibitor, α	1.64	5.69
PLEK[a]	Pleckstrin	1.61	5.24
ZFP36L1	Zinc finger protein 36, C3H type-like 1	1.57	2.72
LTB[a]	Lymphotoxin-β (TNF superfamily, member 3)	1.55	2.13
TNFAIP3[a]	TNFα-induced protein 3	1.50	4.79
GCH1	GTP cyclohydrolase 1 (dopa-responsive dystonia)	1.49	1.62
IRF2	IFN-regulatory factor 2	1.48	2.42
CDKN1B	Cyclin-dependent kinase inhibitor 1B (p27^{Kip1})	1.47	2.23
ANXA7	Annexin A7	1.45	2.76
ARID4B	AT-rich interactive domain 4B (RBP1-like)	1.45	1.78
MARCKS	Myristoylated alanine-rich protein kinase C substrate	1.45	5.60
TRAF3	TNFR-associated factor 3	1.44	1.93
NCOA3	Nuclear receptor coactivator 3	1.41	1.51
PBEF1	Pre-B cell colony-enhancing factor 1	1.41	1.59
PSMB10	Proteasome (prosome, macropain) subunit, β type, 10	1.41	1.42
RUNX3	Runt-related transcription factor 3	1.40	4.13
RNASE3	RNase, RNase A family, 3 (eosinophil cationic protein)	−1.40	−1.49
ADAM28	ADAM metallopeptidase domain 28	−1.41	−1.45
PPIL2	Peptidylprolyl isomerase (cyclophilin)-like 2	−1.45	−1.41
CHRM5	Cholinergic receptor, muscarinic 5	−1.52	−1.64
E2F2	E2F transcription factor 2	−1.54	−1.47

[a] Known NF-κB targets.

up-regulated by both CD40 signal strengths, the serine/threonine kinase *PIM1*, has similarly been linked to apoptosis prevention (23). *PIM1* has also been implicated in the control of the cell cycle, as have three of the other shared genes, *P27KIP1/CDKN1B*, *E2F transcription factor 2* (*E2F2*), and *IFN-regulatory factor 2* (*IRF2*) (24, 25). Of the remaining common genes, many play a role in the internal biochemistry of the cell and/or signal transduction.

For the 20 coordinately up-regulated genes, although the magnitude of increase was invariably greater in cells receiving a strong CD40 signal, differential targeting of genes by the two signal strengths could not be explained by a simple dilution effect. For example, the gene showing the greatest increase in response to strong CD40 signaling, *CD54/ICAM1*, failed to register any change following a weak signal, an outcome that carries through to
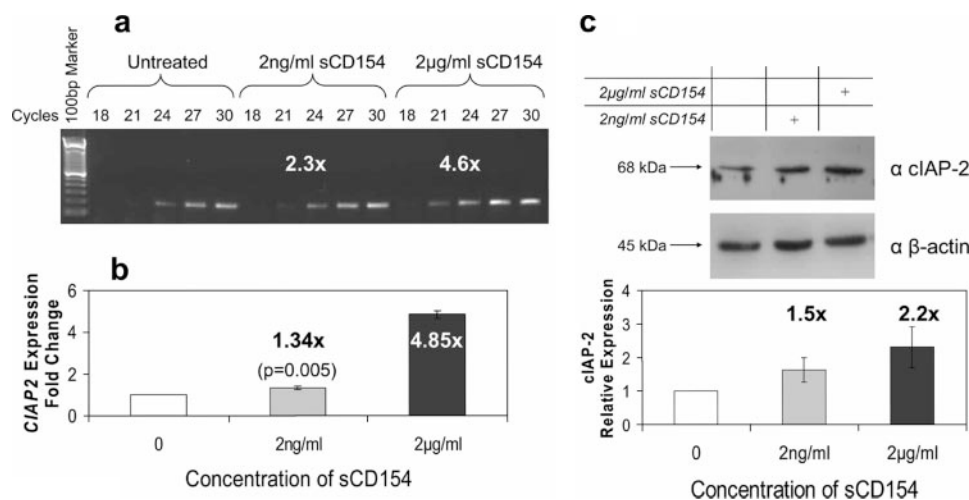

FIGURE 2. Changes in the level of *CIAP2* transcript and protein in L3055 cells following CD40 signals of different strength. L3055 cells were treated with sCD154 at either 2 ng/ml or 2 μg/ml. *a*, cDNA isolated from treated cells after 6 h was used for RT-PCR analysis of *CAIP2* expression. Aliquots of the PCR were taken every three cycles to enable semiquantitation, with β-actin being used to monitor equal cDNA loadings. Similar results were produced from three separate experiments. *b*, The same cDNA was used for quantitative real-time RT-PCR analysis of *CIAP2* expression as described in *Materials and Methods*. Results are ± SEM for three experiments. *c*, Whole-cell lysates were generated from treated cells after 24 h. From each lysate, 30 μg of protein were analyzed by Western blot for cIAP-2 levels (*top*). The amount of cIAP-2 in each sample was quantified by densitometry, normalized against the level of β-actin, and used to calculate expression of cIAP-2 in treated relative to untreated cells (*bottom*). Results are ± SEM for three experiments. α-, Anti-.
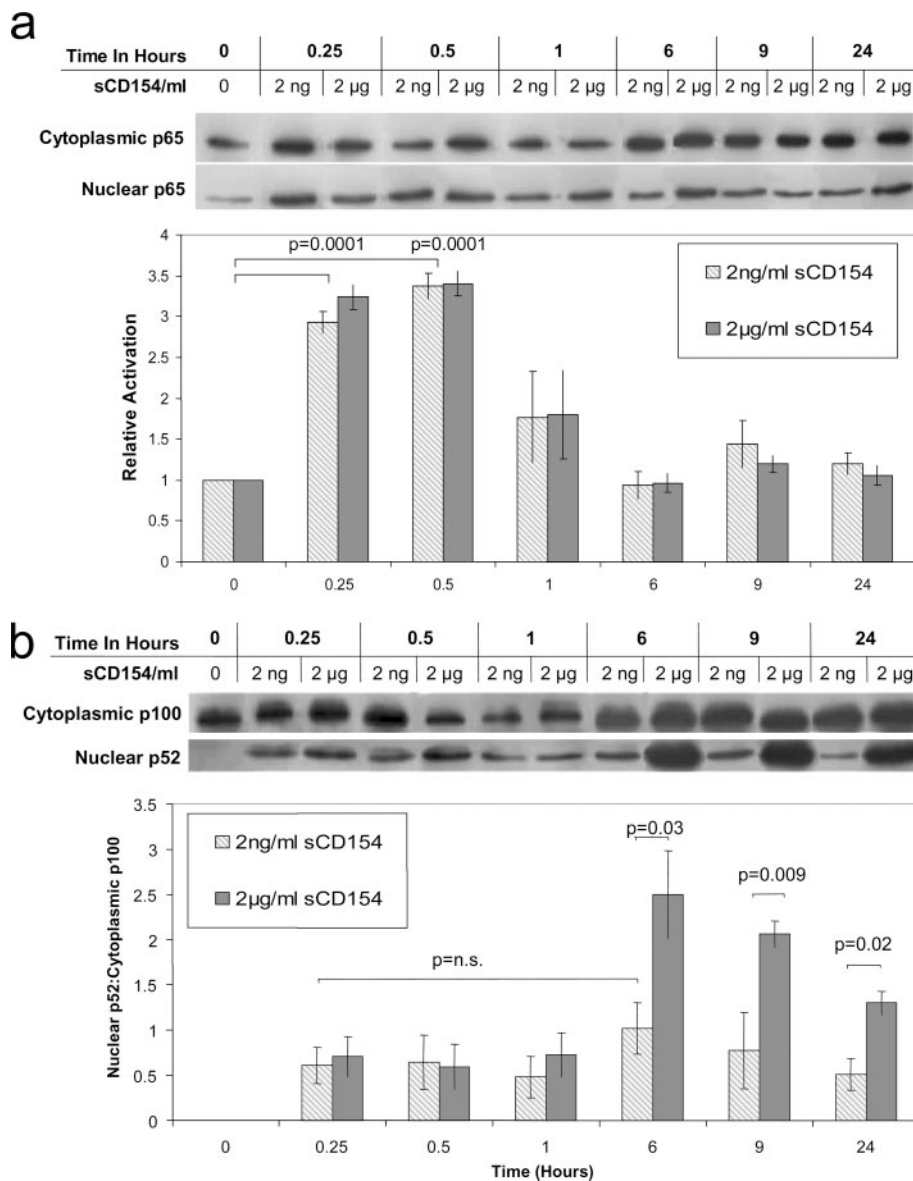
FIGURE 3. Activation of the classical and alternative NF-κB pathways following CD40 signals of different strengths. L3055 cells were cultured together with 2 ng/ml or 2 μg/ml sCD154. Samples were taken after 0.25, 0.5, 1, 6, 9, and 24 h and used to produce cytoplasmic and nuclear lysates. a, Protein, 10 μg from each lysate, was analyzed by Western blot for p65 (*top*). The amount of p65 in each sample was quantified by densitometry, normalized against the level of β-actin and used to calculate the nuclear-cytoplasmic p65 ratio in treated relative to untreated cells. This is expressed as a relative activation compared with resting cells (*bottom*). Results are ± SEM for three experiments. b, Protein, 10 μg from each lysates, was analyzed by Western blot for p100/p52 (*top*). The amount of p100/p52 in each sample was quantified by densitometry, normalized against the level of β-actin and used to calculate the nuclear p52-cytoplasmic p100 ratio in each sample (*bottom*). Results are ± SEM for three experiments.

protein expression (2). Likewise, for the top five genes down-regulated by 2 μg/ml sCD154 (*AID>ID3>MEF2B>BCL6>CD27*), none altered significantly in response to 2 ng/ml ligand.

CIAP2 (BIRC3), the gene showing the highest common change, was selected for validation. First, semiquantitative RT-PCR demonstrated an increase in *CIAP2* transcripts of 2.3-fold and 4.6-fold after 6 h of exposure of L3055 cells to low and high concentrations of sCD154, respectively (Fig. 2). Real-time PCR indicated *CIAP2* up-regulation of 1.3-fold following a weak CD40 signal compared with a 4.8-fold increase on strong CD40-signaling; though seemingly small, the increase on weak signaling was highly significant ($p = 0.005$). Western blotting demonstrated an increase in the level of cIAP-2 protein following both CD40 signal strengths. Quantitation of protein bands by densitometry indicated a 1.5-fold increase following a weak CD40 signal and a 2.2-fold increase following a strong signal (Fig. 2).

Ability of CD40 at different strengths of signaling to engage canonical and alternative arms of the NF-κB pathway

The strong representation of NF-κB targets in the transcriptional analysis above prompted the next set of experiments where activation of this pathway by the two CD40 signal strengths was mea-

sured directly. Western blot showed that both strong and weak signals delivered through CD40 resulted in movement of the p65 subunit of NF-κB into the nucleus of L3055 cells (Fig. 3a). The kinetics of NF-κB pathway activation was compared for L3055 cells encountering low and high CD154 tone. The ratio of nuclear to cytoplasmic p65 was calculated at each time point and used to estimate activation of the classical NF-κB pathway relative to unstimulated cells. Activation of p65 was rapid after delivery of either strength of CD40 signal, reaching 3 times that seen in unstimulated cells within 15 min (Fig. 3a). Activation rose slightly by 30 min, again with both signal strengths achieving comparable levels. By 1 h of incubation with sCD154 (at low or high concentration), the level of p65 activation began to fall, and by 6 h it had returned to that of untreated cells.

The same samples were assessed for activation of the alternative NF-κB pathway using Western blot analysis for p100/p52. No nuclear p52 was seen in unstimulated L3055 cells, and as such it was not possible to calculate relative activation for each sample: instead the ratio of nuclear p52 to cytoplasmic p100 was deduced. Nuclear p52 started to appear in small amounts following CD40 signals of either strength, and it remained relatively low throughout the first hour of culture (Fig. 3b). Six hours after a strong CD40
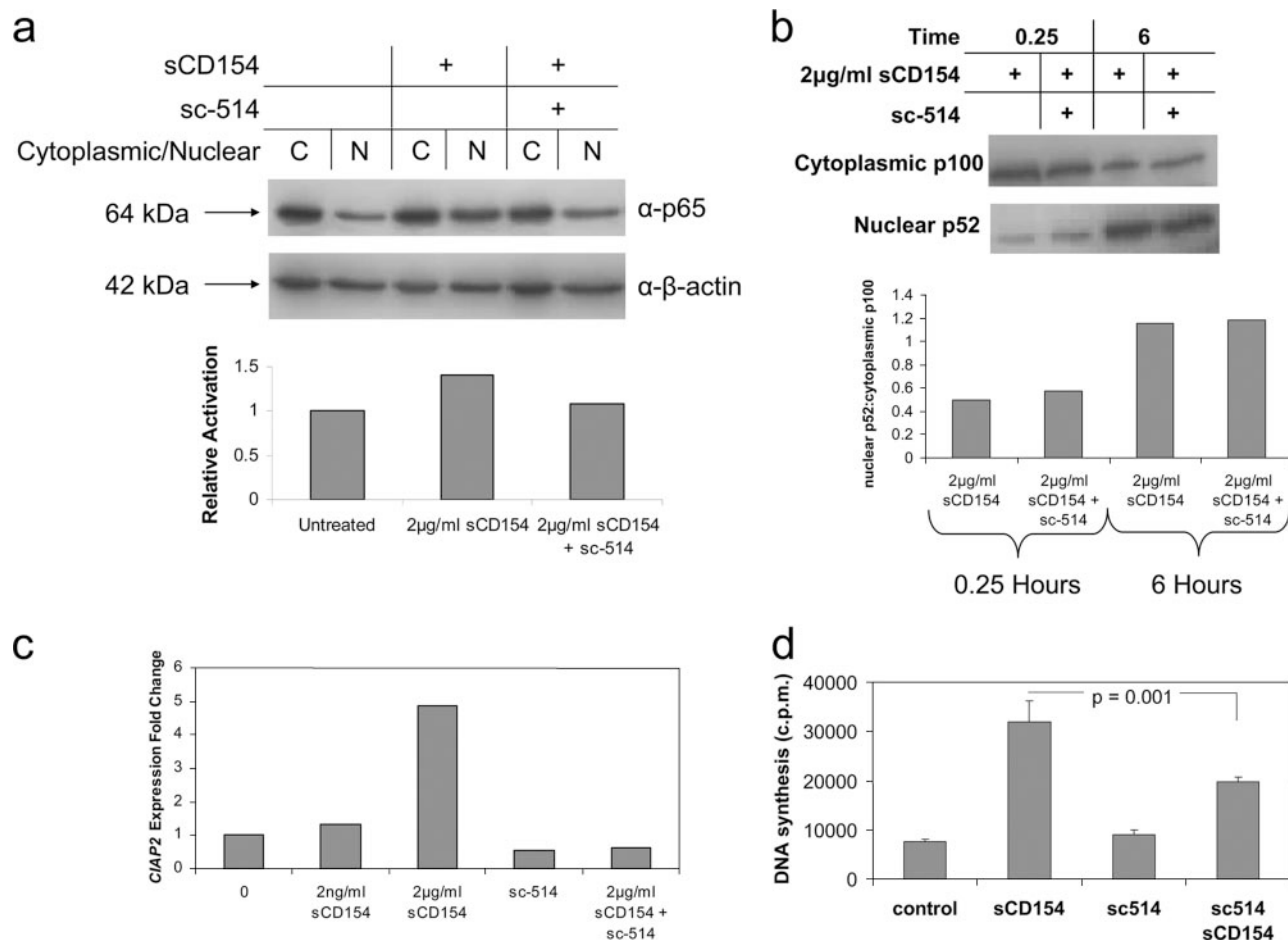
FIGURE 4. CD40-driven changes in NF-κB activation and its effect on gene expression changes. *a*, L3055/Bcl-2 cells were cultured together with 2 μg/ml sCD154 and 100 μM sc-514 as indicated. After 15 min, cytoplasmic (C) and nuclear (N) lysates were isolated and analyzed by Western blot for p65. *b*, L3055/Bcl-2 cells were cultured together with 2 μg/ml sCD154 and 100 μM sc-514 as indicated. After 15 and again after 6 h, cytoplasmic and nuclear lysates were isolated and analyzed by Western blot for p100 and p52. *c*, L3055/Bcl-2 cells were cultured together with 2 μg/ml sCD154 for 6 h, in the presence or absence of 100 μM sc-514. cDNA isolated from these cells was analyzed by real-time RT-PCR for expression of *CIAP2*, as described in *Materials and Methods*. Values are the fold change in expression relative to an untreated control. *d*, L3055 (wild-type) cells at 2000 cells per 200-μl well were preincubated ± 50 μM sc-514 for 1 h followed by treatment ± sCD154 as indicated then cultured for 5 days before pulsing overnight (18 h) with [³H]TdR for determination of DNA synthesis; results given as mean cpm of triplicate determinations ± SEM.

signal the level of nuclear p52 increased dramatically and remained high until at least 9 h. By 24 h of a strong CD40 signal, the level of nuclear p52 had fallen below that at 9 h but was still greater than that seen at earlier time points. In striking contrast to the changes seen following a strong CD40 signal, weak CD154 tone failed to elicit an increase in nuclear p52 significantly above the small early appearance.

As expected, the IKKβ inhibitor sc514 prevented CD40-driven increases in nuclear p65 (Fig. 4*a*) but essentially left the strong CD40-driven accumulation of nuclear p52 unperturbed; indicating that alternative NF-κB pathway activation was independent of the canonical pathway (Fig. 4*b*). Analysis by real-time PCR revealed that inhibition of IKKβ abrogated the CD40-mediated increase in the expression of the antiapoptotic gene *CIAP2* (Fig. 4*c*). CD40-mediated up-regulation of *A20* was similarly affected, whereas down-regulation of the GC signature *BCL6* was attenuated by 90% (data not shown). IKKβ inhibition similarly reversed the majority of the maintenance capacity of 2 ng/ml sCD154 for L3055 cells otherwise dying from low-density seeding, although having no effect on basal proliferation (Fig. 4*d*). Bay 11-7082, an inhibitor of IKBα phosphorylation, was found to be directly antiproliferative and proapoptotic for L3055 cells when used at concentrations required to block NF-κB activation (0.5–10 μM; data not detailed).

Discussion

It is now accepted that CD40-CD154 encounters are set more like a rheostat than an on/off switch (26), with CD40L functioning in a graded manner (5). How ligand availability translates to assorted outcomes has been unclear. Here we have identified a differential capacity to engage the alternative NF-κB axis as a potential discriminator to the downstream consequences of low vs high level CD40 signaling.

A major aim of this study was to tease out from the myriad of targets potentially impacted by CD40, a survival signature that in turn might disclose unique or restricted pathways to this phenotype, critical not only in physiological B cell homeostasis but also in lymphomagenesis and potentially other immune disturbances. There is increasing evidence that lymphoma pathology is contributed by TNF family ligands (27, 28). In BL, a prototypic GC malignancy, autonomous survival can be instigated by CD154 produced in response to population depletion (2). For large B cell lymphoma, constitutive *CD154* activation leads to the formation of a CD40-dependent signalosome (4, 28). We have previously detailed the markers of differentiation, changes in morphology/adhesion, and the growth arrest that accompany survival in BL cells on saturating surface membrane CD40 with cognate ligand (2, 6). The

lack of these indicators on delivering amounts of CD154 that, although low, still suppress apoptosis allowed for discriminatory exploration of pathways generating restricted (survival) and multiple outcomes, respectively.

The strong representation of NF-κB targets among genes changing coordinately in response to weak and strong ligand tone posited this pathway as a candidate for delivering CD40-dependent survival to L3055 cells. Of the nine shared genes increasing ≥1.5-fold on low-level CD40 occupancy, all but two fell within the NF-κB-dependent cluster. Most have been linked to CD40 signaling including that resulting in survival with *CIAP2*, *A20*, *IKBA*, and *TANK* of particular note (18, 19). Direct measurement of NF-κB activation revealed rapid engagement of the canonical pathway by weak and strong CD40 signals equally, whereas its inhibition abrogated CD40-driven increases in the survival signatures *CIAP2* and *A20*. A recent study comparing NF-κB-inhibited genes in lymphoma lines infected with EBV and Kaposi's sarcoma herpesvirus, respectively, disclosed only 25 (from 12,500 analyzed) overlapping between the two. Among these were *CIAP2* and *A20*, as well as *IKBA*: neither *BCL2* nor *Bcl-xL* registered despite the profound impact of NF-κB inhibition on lymphoma cell survival in that study (29). Thus, on distinct backgrounds and in different maintenance contexts (virally promoted vs CD40-signaled as here) remarkably consistent NF-κB targets appear to be associated with a survival signature.

An interesting finding of the present study was the indication of a diverging capacity between strong and weak CD40 signals to engage the alternative NF-κB pathway. Robust noncanonical NF-κB activation, observed only on strong CD40 signaling, was significantly delayed compared with rapid canonical pathway engagement by both signal strengths. Such delay would, teleologically, render the alternative pathway redundant with regards a survival response which must be met early for the cell to continue. Early canonical NF-κB activation did not appear essential to later engagement of the alternative pathway, the latter still proceeding in the presence of the selective IKKβ inhibitor, sc-514. The capacity of sc-514 to abrogate up-regulation of *CIAP2* and *A20* while substantially reversing low-level CD40 maintenance of L3055 cell cultures supports the notion that the classical arm of the NF-κB pathway selectively contributes these outcomes. For murine B cells, CD40 is capable of conferring some survival even where both routes to NF-κB activation have been ablated: seemingly by up-regulating Bcl-x$_L$ (30). This apparent discrepancy could reflect a difference in the maintenance requirements between quiescent and proliferating B cells. CD40-driven proliferation (and the induction of proliferation-related genes) in murine B cells required an intact canonical pathway whereas the alternative NF-κB pathway was redundant in this regard (30).

It is of interest to compare the CD40-promoted transcriptome changes in L3055 cells with those described in other B cell backgrounds. The closest comparator is probably that from Basso et al. (31), in which, to establish a baseline for tracking CD40 signatures during a GC response, they first undertook transcriptional profiling on the Ramos BL line. Although their study extended to 24 h and used CD154-transfected fibroblasts to deliver the CD40 signal, common themes emerge. These include: down-regulation of *BCL6*; increases in MHC class II genes; up-regulation of *CD40*, *LTA*, and *LTB*; increases in multiple NF-κB-dependent genes including those encoding A20, TRAF1, and PI-3K. Many of these genes also appeared in a study profiling murine B cells stimulated with soluble CD154 fusion protein (32).

The capacity of a single receptor to convey disparate signaling information depending on engagement thresholds is not unique, even among the TNFR family, including CD40 itself. In murine macrophages, a weak CD40 signal drives ERK1/2-dependent IL-10 expression whereas stronger signals promote p38^{MAPK}-dependent IL-12 production (33). The level of CD95 available for engagement can similarly set subsequent signaling and functional consequences: a reduced complement of receptor, as occurs in a subset of patients with autoimmune lymphoproliferative syndrome, resulting in efficient (canonical) NF-κB activation but not apoptosis whereas normal levels signal both (34).

A major question now is how sensing by CD40 of shifting ligand availability at the B cell surface is translated to discriminatory engagement of the separate routes to NF-κB activation, thereby limiting, or extending, functional sequelae. TRAF family members may be arbiters here. Inhibition of TRAF2/5 by TRAF3 downstream of CD40 can selectively inhibit alternative NF-κB pathway activation while leaving the classical pathway intact (35). In L3055 cells, *TRAF3* was up-regulated following a weak CD40 signal in the absence of expression change in other TRAFs. Possibly, up-regulation of TRAF3 alone in this context represses the activation of the alternative NF-κB pathway that is seen following a strong CD40 signal. Conversely, rendering murine B cells TRAF2 deficient reveals its requirement for CD40 linking to the canonical pathway while making them constitutively hyperactive for the alternative NF-κB pathway (36). CD40 signaling promotes rapid ubiquitin-targeted degradation of TRAF2, thereby generating the potential conditions for noncanonical NF-κB activation. In contrast with what is observed on strong CD40 signaling, we have failed to register in L3055 cells any modification to TRAF2 following low-level engagement of CD40 (A. Chamba and J. Gordon, unpublished observations). A comprehensive analysis of TRAF requirement, recruitment, and modification in response to varying levels of CD40 occupancy may disclose attractive candidates for the selective disruption of NF-κB-dependent survival in lymphoma that exploit autonomous CD154 to this end. Common pathways may operate in maintaining polyreactive B cell clones in a non-cell-autonomous manner (5); these may prove equally amenable to targeting in the context of autoimmunities such as lupus and other autoantibody-mediated diseases. Clearly, the principles established here in model BL cells should now be addressed in their physiological GC B cell counterparts (i.e., centroblasts) in which minimal CD40 engagement is likewise sufficient to rescue from apoptosis (37) with ligand being delivered, potentially, via low-level autonomous provision (38). Although this study has focused on the signals and genes associated primarily with the survival phenotype engendered by low-level CD40 receptor occupancy which may pertain equally to the L3055 lymphoma cell model and normal GC B cell subsets, it will also be of interest in future experiments to address outcomes that are selective to high-level CD40 engagements; and perhaps to lymphoma cell dynamics, as indicated by the growth arrest specifically observed when such populations are presented with a strong CD154 signal (1, 6).

Disclosures
The authors have no financial conflict of interest.

References

1. Gordon, J., and J. D. Pound. 2000. Fortifying B cells with CD154: an engaging tale of many hues. *Immunology* 100: 269–280.
2. Challa, A., A. G. Eliopoulos, M. J. Holder, A. S. Burguete, J. D. Pound, A. Chamba, G. Grafton, R. J. Armitage, C. D. Gregory, H. Martinez-Valdez, et al. 2002. Population depletion activates autonomous CD154-dependent survival in biopsylike Burkitt lymphoma cells. *Blood* 99: 3411–3418.
3. Siddiqa, A., J. C. Sims-Mourtada, L. Guzman-Rojas, R. Rangel, C. Guret, V. Madrid-Marina, Y. Sun, and H. Martinez-Valdez. 2001. Regulation of CD40

and CD40 ligand by the AT-hook transcription factor AKNA. *Nature* 410: 383–387.

4. Pham, L. V., A. T. Tamayo, L. C. Yoshimura, P. Lo, N. Terry, P. S. Reid, and R. J. Ford. 2002. A CD40 signalosome anchored in lipid rafts leads to constitutive activation of NF-κB and autonomous cell growth in B cell lymphomas. *Immunity* 16: 37–50.

5. Lesley, R., L. M. Kelly, Y. Xu, and J. G. Cyster. 2006. Naïve CD4 T cells constitutively express CD40L and augment autoreactive B cell survival. *Proc. Natl. Acad. Sci. USA* 28: 10717–10722.

6. Baker, M. P., A. G. Eliopoulos, L. S. Young, R. J. Armitage, C. D. Gregory, and J. Gordon. 1998. Prolonged phenotypic, functional, and molecular change in group I Burkitt lymphoma cells on short-term exposure to CD40 ligand. *Blood* 92: 2830–2843.

7. Irizarry, R. A., B. M. Bolstad, F. Collin, L. M. Cope, B. Hobbs, and T. P. Speed. 2003. Summaries of Affymetrix GeneChip probe level data. *Nucleic Acids Res.* 31: E15.

8. Gautier, L., L. Cope, B. M. Bolstad, and R. A. Irizarry. 2004. Affy-analysis of Affymetrix GeneChip data at the probe level. *Bioinformatics* 20: 307–315.

9. Storey, J. D., and R. Tibshirani. 2003. Statistical methods for identifying differentially expressed genes in DNA microarrays. *Methods Mol. Biol.* 224: 149–157.

10. Donahue, A. C., and D. A. Fruman. 2004. PI3K signaling controls cell fate at many points in B lymphocyte development and activation. *Semin. Cell Dev. Biol.* 15: 183–197.

11. Brennan, P., A. M. Mehl, M. Jones, and M. Rowe. 2002. Phosphatidylinositol 3-kinase is essential for the proliferation of lymphoblastoid cells. *Oncogene* 21: 1263–1271.

12. Agematsu, K. 2000. Memory B cells and CD27. *Histol. Histopathol.* 15: 573–576.

13. Fukuda, T., T. Miki, T. Yoshida, M. Hatano, K. Ohashi, S. Hirosawa, and T. Tokashisu. 1995. The murine *BCL6* gene is induced in activated lymphocytes as an immediate early gene. *Oncogene* 11: 1657–1663.

14. A. Durandy. 2003. Activation-induced cytidine deaminase: a dual role in class-switch recombination and somatic hypermutation. *Eur. J. Immunol.* 33: 2069–2073.

15. Yim, J. H., S. H. Ro, J. K. Lowney, S. J. Wu, J. Connett, and G. M. Doherty. 2003. The role of interferon regulatory factor-1 and interferon regulatory factor-2 in IFN-γ growth inhibition of human breast carcinoma cell lines. *J. Interferon Cytokine Res.* 23: 501–511.

16. Shimizu, M., Y. Nomura, H. Sukuki, E. Ichikawa, A. Takeuchi, M. Suzuki, T. Nakamura, T. Nakajima, and K. Oda. 1998. Activation of the rat cyclin A promoter by ATF2 and Jun family members and its suppression by ATF4. *Exp. Cell Res.* 239: 93–103.

17. Muller, H. J., C. Skerka, A. Bialonski, and P. F. Zipfel. 1991. Clone pAT 133 identifies a gene that encodes another human member of a class of growth factor-induced genes with almost identical zinc-finger domains. *Proc. Natl. Acad. Sci. USA* 88: 10079–10083.

18. Song, H. Y., M. Rothe, and D. V. Goeddel. 1996. The tumor necrosis factor-inducible zinc finger protein A20 interacts with TRAF1/TRAF2 and inhibits NF-κB activation. *Proc. Natl. Acad. Sci. USA* 93: 6721–6725.

19. Chariot, A., A. Leonardi, J. Muller, M. Bonif, K. Brown, and U. Siebenlist. 2002. Association of the adaptor TANK with the I κB kinase (IKK) regulator NEMO connects IKK complexes with IKKε and TBK1 kinases. *J. Biol. Chem.* 277: 37029–37036.

20. Sarma, V., Z. Lin, L. Clark, B. M. Rust, M. Tewari, R. J. Noelle, and V. M. Dixit. 1995. Activation of the B-cell surface receptor CD40 induces A20, a novel zinc finger protein that inhibits apoptosis. *J. Biol. Chem.* 270: 12343–12346.

21. Craxton, A., G. Shu, J. D. Graves, J. Saklatvala, E. G. Krebs, and E. A. Clark. 1998. p38 MAPK is required for CD40-induced gene expression and proliferation in B lymphocytes. *J. Immunol.* 161: 3225–3236.

22. Fotin-Mleczek, M., F. Henkler, A. Hausser, H. Glauner, D. Samel, A. Graness, P. Scheurich, D. Mauri, and H. Wajant. 2004. Tumor necrosis factor receptor-associated factor (TRAF) 1 regulates CD40-induced TRAF2-mediated NF-κB activation. *J. Biol. Chem.* 279: 677–685.

23. Bachmann, M., and T. Moroy. 2005. The serine/threonine kinase Pim-1. *Int. J. Biochem. Cell Biol.* 37: 726–730.

24. Sgambato, A., A. Cittadini, B. Faraglia, and I. B. Weinstein. 2000. Multiple functions of p27^{Kip1} and its alterations in tumor cells: a review. *J. Cell Physiol.* 183: 18–27.

25. Fang, Z. H., and Z. C. Han. 2006. The transcription factor E2F: a crucial switch in the control of homeostasis and tumorigenesis. *Histol. Histopathol.* 21: 403–413.

26. Neron, S., C. Racine, A. Roy, and M. Guerin. 2005. Differential responses of human B-lymphocyte subpopulations to graded levels of CD40-CD154 interaction. *Immunology* 116: 454–463.

27. Mackay, F., and S. G. Tangye. 2004. The role of the BAFF/APRIL system in B cell homeostasis and lymphoid cancers. *Curr. Opin. Pharmacol.* 4: 347–354.

28. Pham, L. V., A. T. Tamayo, L. C. Yoshimura, Y. C. Lin-Lee, and R. J. Ford. 2005. Constitutive NF-κB and NFAT activation in aggressive B cell lymphomas synergistically activates the CD154 gene and maintains lymphoma cell survival. *Blood* 106: 3940–3947.

29. Keller, S. A., D. Hernandez-Hopkins, J. Vider, V. Ponomarev, E. Hyjek, E. J. Schattner, and E. Cesarman. 2006. NF-κB is essential for the progression of KSHV- and EBV-infected lymphomas in vivo. *Blood* 107: 3295–3302.

30. Zarnegar, B., J. Q. He, G. Oganesyan, A. Hoffmann, D. Baltimore, and G. Cheng. 2004. Unique CD40-mediated biological program in B cell activation requires both type 1 and type 2 NF-κB activation pathways. *Proc. Natl. Acad. Sci. USA* 101: 8108–8113.

31. Basso, K., U. Klein, H. Niu, G. A. Stolovitzky, Y. Tu, A. Califano, G. Cattoretti, and R. Dalla-Favera. 2004. Tracking CD40 signaling during germinal center development. *Blood* 104: 4088–4096.

32. Dadgostar, H., B. Zarnegar, A. Hoffmann, X. F. Qin, U. Truong, G. Rao, D. Baltimore, and G. Cheng. 2002. Cooperation of multiple signaling pathways in CD40-regulated gene expression in B lymphocytes. *Proc. Natl. Acad. Sci. USA* 99: 1497–1502.

33. Mathur, R. K., A. Awasthi, P. Wadhone, B. Ramanamurthy, and B. Saha. 2004. Reciprocal CD40 signals through p38MAPK and ERK-1/2 induce counteracting immune responses. *Nat. Med.* 10: 540–544.

34. Legembre, P., B. C. Barnhart, L. Zheng, S. Vijayan, S. E. Straus, J. Puck, J. K. Dale, M. Lenardo, and M. E. Peter. 2004. Induction of apoptosis and activation of NF-κB by CD95 require different signalling thresholds. *EMBO Rep.* 5: 1084–1089.

35. Hauer, J., S. Puschner, and P. Ramakrishnan. 2005. TNF receptor (TNFR)-associated factor (TRAF) 3 serves as an inhibitor of TRAF2/5-mediated activation of the noncanonical NF-κB pathway by TRAF-binding TNFRs. *Proc. Natl. Acad. Sci. USA* 102: 2874–2879.

36. Grech, A. P., M. Amesbury, T. Chan, S. Gardam, A. Basten, and R. Brink. 2004. TRAF2 differentially regulates the canonical and noncanonical pathways of NF-κB activation in mature B cells. *Immunity* 21: 629–642.

37. Pound, J. D., A. Challa, M. J. Holder, R. J. Armitage, S. K. Dower, W. C. Fanslow, H. Kikutani, S. Paulie, C. D. Gregory, and J. Gordon. 1999. Minimal cross-linking and epitope requirements for CD40-dependent suppression of apoptosis contrast with those for the promotion of the cell cycle and homotypic adhesions in human B cells. *Int. Immunol.* 11: 11–20.

38. Grammer, A. C., R. D. McFarland, J. Heaney, B. F. Darnell, and P. E. Lipsky. 1999. Expression, regulation, and function of B-cell expressed CD154 in germinal centers. *J. Immunol.* 163: 4150–4159.